Molecular determinants of membrane potential dependence in vertebrate gap junction channels

Ana Revilla[†], Michael V. L. Bennett[‡], and Luis C. Barrio[†§]

[†]Neurología Experimental-Unidad Asociada al Consejo Superior de Investigaciones Científicas, Departamento de Investigación, Hospital ''Ramón y Cajal,'' Carretera de Colmenar Viejo km. 9, 28034 Madrid, Spain; and [‡]Department of Neuroscience, Albert Einstein College of Medicine, 1300 Morris Park Avenue, Bronx, NY 10461

Contributed by Michael V. L. Bennett, October 6, 2000

The conductance, g_j, of many gap junctions depends on voltage between the coupled cells (transjunctional voltage, V_j) with little effect of the absolute membrane potential (V_m) in the two cells; others show combined V_j and V_m dependence. We examined the molecular determinants of V_m dependence by using rat connexin 43 expressed in paired *Xenopus* oocytes. These junctions have, in addition to V_j dependence, V_m dependence such that equal depolarization of both cells decreases g_j. The dependence of g_j on V_m was abolished by truncation of the C-terminal domain (CT) at residue 242 but not at 257. There are two charged residues between 242 and 257. In full-length Cx43, mutations neutralizing either one of these charges, Arg243Gln and Asp245Gln, decreased and increased V_m dependence, respectively, suggesting that these residues are part of the V_m sensor. Mutating both residues together abolished V_m dependence, although there is no net change in charge. The neutralizing mutations, together or separately, had no effect on V_j dependence. Thus, the voltage sensors must differ. However, V_j gating was somewhat modulated by V_m, and V_m gating was reduced when the V_j gate was closed. These data suggest that the two forms of voltage dependence are mediated by separate but interacting domains.

Gap junction channels are unique among ionic channels in that they span two cell membranes. They are composed of two hemichannels, one in each membrane, that are tightly docked head to head to form a pore that directly connects the cytoplasm of two cells (1). In vertebrates, gap junctions are formed by connexins (Cx), a gene family of protein subunits (2). Given their architecture, gap junction channels are subject to the influence of two types of voltage, that between the two cell interiors termed transjunctional voltage (V_j), and that between the interior and exterior or the membrane potential (V_m), which can differ between the cells and thus along the lumen of the channel connecting the cells. Many gap junctions are sensitive to V_j with little effect of V_m, whereas others show combined V_j and V_m dependence. The eponymous gap is accessible to small ions and because there is negligible leak through the channel wall, the potential in the gap is likely to be close to that in the bathing medium (3). V_m dependence of junctional conductance (g_j) was initially described in invertebrate (deuterostome) gap junctions (4–7), which are formed by innexins, a family of proteins unrelated to connexins (8). More recently, g_j dependence of V_m has also been demonstrated in junctions formed of vertebrate connexins in exogenous expression systems (9–11) as well as in native cells (12, 13). Junctions comprised of different connexin isoforms have divergent properties of V_m dependence, varying in their polarity of closing, voltage sensitivity, and kinetics (14).

V_j dependence of vertebrate gap junctions has been extensively analyzed by site-directed mutagenesis (15–18), but the molecular basis of V_m gating remains unknown. There is increasing evidence that separate gates mediate V_m and V_j dependence, a hypothesis supported by the striking differences in the gating induced by the two types of potential (14) and by the divergent evolution of their properties among Cx45 junctions in different vertebrate classes (10). Because the junctional conductance of rat Cx43 channels shows sensitivity to V_m as well as V_j, we chose to study the molecular determinants for V_m regulation in these channels. Cx43 is perhaps the most abundant gap junction protein and is widely distributed in vertebrate cells and tissues (19), being a major component of intercellular channels between cardiac myocytes, astrocytes, and uterine smooth muscle cells. In the present study, we have identified two charged amino acids located at the most proximal region of the carboxyl-terminal domain (CT) that are likely to be an integral part of the V_m sensor. Mutations of these residues altered V_m dependence markedly but had no effect on V_j dependence. From these and previously reported data, a model was derived with fast and slow V_j gates and a V_m gate in each hemichannel.

Materials and Methods

Mutagenesis and Channel Expression in Paired Oocytes. The mutants (G242stop, R243Q, and D245Q) were constructed by PCR mutagenesis of rat Cx43 cDNA, as previously described for rat Cx43 truncated at position 257 (S257stop; ref. 18), using the following primers: G242stop, sense 5′-TGATATCCGAGCTGTCGATTATGGAGGAGA-3′ that created a new *Eco*RV site, and antisense 5′-CTTCACGCGATCCTTAACGCCTTTGAAGAA-3′; R243Q, sense 5′-GATCCTTACCACGCCACCACTGGCCC-3′, and antisense 5′-CGATTGTCCCTTCTTCACGCGATCCTTAAC-3′, which in combination created a new *Bam*HI site; D245Q, sense 5′-AGATCTCAGCCTTACCACGCCACCACTGGC-3′, and antisense 5′-TCTTCCCTTCACGCGATCCTTAACGCC T-3′, which introduced a new *Bgl*II site. The mutant carrying the double R243Q and D245Q substitution was obtained by using the D245Q mutant as template and the following primers: sense 5′-AGATCTCAGCCTTACCACGCCACCACTGGC-3′ and antisense 5′-TTGTCCCTTCACGCGATCCTTAACGCCT-3′, which destroyed the *Bgl*II site created in the D245Q construct. The cRNA synthesis and purification were performed as previously described (18). Oocytes were removed from the ovaries of *Xenopus laevis* (African *Xenopus* Facility, South Africa) under anesthesia and prepared as described (13).

Electrophysiology and Data Analysis. The macroscopic junctional conductance (g_j) between the paired oocytes injected with cRNAs (0.1–0.5 μg/μl; 50 nl/oocyte) and an antisense directed against *Xenopus* Cx38 mRNA (10 ng/oocyte; ref. 20) were measured with the dual voltage clamp technique (21). The influence of V_m on g_j was explored by applying equal displacements of the membrane potential in both cells of a pair (V_1 and V_2) while g_j was monitored

Abbreviations: Cx, connexin; g_j, junctional conductance; V_m, membrane potential; V_j, transjunctional voltage; CT, carboxyl-terminal domain; WT, wild type.

[§]To whom reprint request should be addressed. E-mail: luis.c.barrio@hrc.es.

The publication costs of this article were defrayed in part by page charge payment. This article must therefore be hereby marked "*advertisement*" in accordance with 18 U.S.C. §1734 solely to indicate this fact.

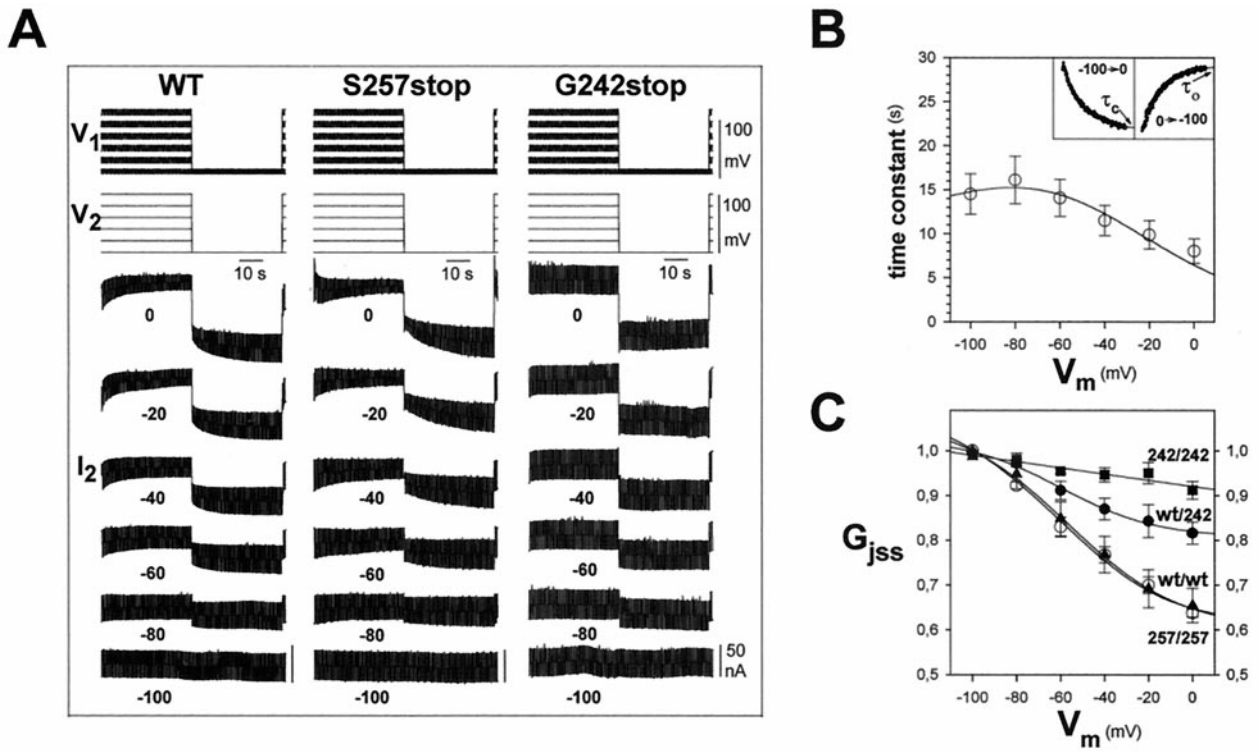

Fig. 1. Localization of the V_m determinants in the CT domain of rat Cx43. WT and the Cx43 channels truncated at positions S257stop and G242stop were expressed in *Xenopus laevis* oocytes pairs. *(A)* Sample records of nonjunctional and junctional currents (I_2) induced by the equal displacement of membrane potentials in the two cells (V_1 and V_2; steps of 40 s from −100 to 0 mV in increments of 20 mV, returning to −100 mV for 40 s between each step). The junctional currents (I_j) measured in oocyte 2 after application of small V_j pulses in oocyte 1 (+10 mV, 500 ms, 1 Hz). For WT (left) and S257stop (center) junctions, I_j decreased on depolarization, more rapidly and to progressively lower steady state values as more positive potentials were achieved. I_j recovered to its initial values on returning to −100 mV. The mutation G242stop largely abolished the dependence of junctional conductance (g_j) on V_m (right). (*B*) V_m dependence of the time constant of decrease in g_j. The time course of relaxations to G_{jss} was well fit by single exponentials (*Inset*) with long time constants that were shorter at more positive voltages. The smooth curve is derived from calculations assuming a single Boltzmann model. (*C*) Graphs of G_{jss}/V_m relations where G_{jss} is normalized to the value at −100 mV. The smooth curves are derived from fits to the square of a Boltzmann relation based on a model of two independent gates in series, one in each hemichannel (except for WT-G242stop, for which a single Boltzmann and gate were assumed). The parameters are given in Table 1. The G_{jss} of WT (○) and truncated S257stop (▲) junctions decreased by ≈50% when V_m increased from −100 to 0 mV. G_{jss} of truncated G242stop junctions (■) was quite insensitive to V_m. The G_{jss}/V_m curve of hybrid WT-G242stop junctions (●) was in between those of the homotypic junctions of the component combinations, suggesting that only the V_m gate of WT hemichannels contributed to their V_m dependence. Each point in *B* represents mean values (±SEM) of six pairs.

by test V_j pulses (10 mV, 500 ms, 1 Hz), too small and brief to induce changes in g_j. The V_j pulses were created by voltage steps in cell 1, and defined as $V_j = V_1 - V_2$, whereas currents injected in cell 2 to hold its potential constant were equal in magnitude and opposite in sign to the currents flowing through the junctional channels (I_j). Voltages and currents in cell 1 and 2 are displayed positive up so that I_j in cell 2 is downward for positive V_j in Figs. 1 and 2. Because total current in cell 2 was the sum of junctional (I_j) and sometimes slowly changing nonjunctional (I_{nj}) currents induced by the simultaneous application of the V_m step and the V_j pulses, the junctional current in Fig. 3*C* was calculated as $I_j = I_2(V_j = 10\ \text{mV}) - I_2(V_j = 0)$ measured at the center of each V_j pulse and at the center of the next interpulse interval. For this figure, I_j is plotted positive up. g_j was calculated as I_j/V_j. Influence of V_j on g_j (Fig. 3*B*) was characterized as in Revilla *et al.* (18). Stimulation and data collection were performed as previously described (10, 18).

Steady state g_j values (g_{jss}) measured at the end of V_j pulses were normalized relative to the g_j value for brief V_j prepulses (10 mV), and the G_{jss}/V_j relation was modeled according to the two-state Boltzmann model (21). In the V_m protocols, g_{jss} was normalized to its value at a holding potential of −100 mV to give G_{jss}, which was plotted as a function of V_m. To analyze the V_m data, we assumed two independent V_j gates in series, one per hemichannel (5, 10, 14). We also assumed that each gate could be either open or completely closed and that for each gate the steady state probability that it was open, p_{oss}, was given by a Boltzmann relation of the form:

$$P_{oss} = \{(P_{omax} - P_{omin})/(1 + \exp[A(V_m - V_0)])\} + P_{omin}$$

where P_{omax} and P_{omin} are the maximum and minimum values of P_o, V_0 is the voltage at which $P_{oss} = (P_{omax} - P_{omin})/2 + P_{omin}P$, A [A = nq/kT] is a constant that expresses the voltage sensitivity in terms of gating charge, the equivalent number (n) of electron charges (q) moving through the entire membrane voltage, and kT has its usual significance. Junctions with a single functional V_m gate on one side, i.e., junctions formed of wild-type (WT) Cx43 on one side and a truncation mutant lacking V_m dependence on the other side are described below. For these junctions, P_o times N, the number of channels, times γ, the single channel conductance, gives g_j, and after normalization:

$$G_{jss} = \{(G_{jmax} - G_{jmin})/(1 + \exp[A(V_m - V_0)])\} + G_{jmin}$$

where G_{jss} is the normalized steady state value as a function of V_m, G_{jmax} is the maximum steady state conductance, and G_{jmin} is the residual conductance or V_m insensitive component. The same form of the equation applies to the situation where the channel closes to a substate, γ_s, rather than to a non-zero P_o. Parameters of voltage dependence were determined by treating G_{jmax}, G_{jmin}, A, and V_0 as free parameters and applying an iterative procedure of fitting (10). The time course of g_j transi-

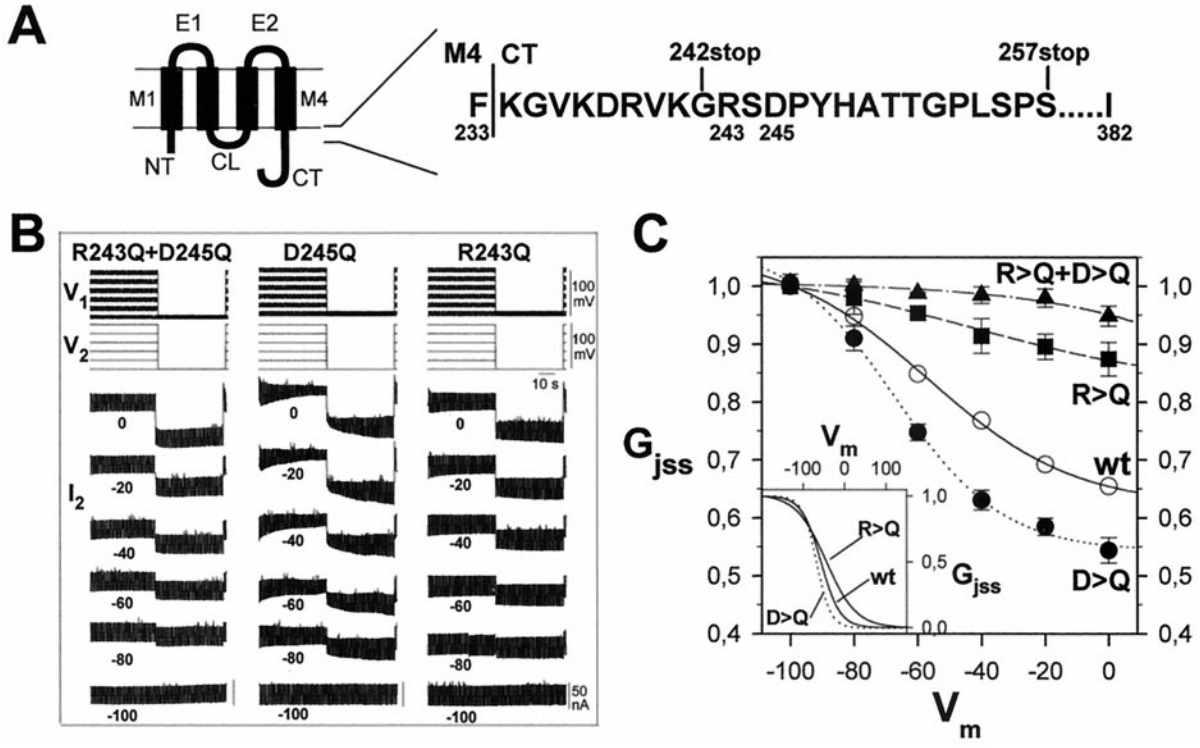

Fig. 2. Effects of mutations R243Q and D245Q on V_m gating. *(A)* Diagram of the topology of connexins (left). There are four transmembrane domains (M1–M4), two extracellular (E1, E2), cytoplasmic N- and C-terminal (NT, CT), and a cytoplasmic loop (CL). Amino acid sequence of the CT at its border with M4 (right) showing sites of the truncation mutants. The region between residues 242 and 257 contains one positively charged residue, Arg-243, and one negatively charged residue, Asp-245. *(B)* Sample records of nonjunctional and junctional currents as in Fig. 1 for mutants carrying single and double neutralizations (R243Q+D245Q, left; D245Q, center; and R243Q, right). The double mutation virtually abolished V_m sensitivity. The single mutations, D245Q and R243Q, increased and reduced dependence of g_j on V_m, respectively. *(C)* Graphs of G_{jss}/V_m relations. The curves are fits of the squared Boltzmann relations with parameters of Table 1. The g_j of junctions carrying the double R243Q+D245Q neutralization (▲) was not V_m sensitive. The single mutations, R243Q (■, broken line) and D245Q (●, dotted line), altered in opposite directions the steepness of V_m gating relative to WT (○, continuous line). The mutations also produced corresponding changes in V_0, the voltage for half change in the V_m sensitive component, relative to WT (*Inset*). Each point in *C* represents mean values (±SEM) of six pairs.

tions was fitted with exponentials with $R > 0.999$ by using CLAMPFIT (pCLAMP, Axon, CA) and the τ/V_m relation calculated from the equations derived from first-order kinetics (22).

The model differs somewhat for channels that have two functional V_m gates and zero conductance if one or both of the V_m gates is closed, i.e., the closed gates do not have a finite residual conductance (we will justify this assumption in the presentation of Fig. 3). In this case, the open probability will be given by the square of Boltzmann relation for the single gate:

$$P_o = \{(P_{omax} - P_{omin})/(1 + \exp[A(V_m - V_0)]) + P_{omin}\}^2$$

where P_o is the steady state open probability of the channel, and P_{omax} and P_{omin} are the limiting values of the open probabilities for the two series gates. If P_{omax} approaches 1, P_{omin} will be given by $(G_{jmin}/G_{jmax})^{1/2}$.

Results

Localization of Molecular Determinants for V_m Gating in the Cx43 Molecule. Rat connexin 43 junctions exhibit combined membrane potential (V_m) and transjunctional voltage (V_j) dependence of junctional conductance, g_j (9, 18). The V_m dependence of g_j was explored independently of V_j dependence by applying equal displacements of the membrane potential in two cells of a coupled pair. With $V_j = 0$, increasing depolarizing steps applied to both cells induced progressive reduction in g_j. On returning to the holding potential of −100 mV, g_j recovered its initial value (Fig. 1*A* WT). The steady state G_j/V_m curve was well described by the square of a Boltzmann relation (Fig. 1*C*, Table 1), a calculation based on the assumption that there are two identical but independent V_m gates in series, one per hemichannel. Over the range of membrane potentials explored, G_{jss} changed ≈80% of the difference between the extrapolated values of G_{jmax} and G_{jmin}. Decay and recovery of g_j in response to application of V_m were monotonic and approximately exponential, with time constants of several seconds (Fig. *1B*). We did not attempt to fit the time course data with a squared Boltzmann relation.

It has been previously reported that the g_j transitions induced by V_j in RCx43 junctions have fast and slow components, the fast component being larger at larger V_j (≈80% at $V_j = -100$ mV). Truncation of the CT domain by the mutation S257stop alters the transitions; there is a single component of decay in g_j with a time constant somewhat shorter than that of the slow component of WT junctions (18). V_m dependence of G_{jss} of S257stop–S257stop junctions was virtually identical to that of the WT channels (Fig. 1*A* S257stop and 1*C*; Table 1), indicating that residues 257–382 of the CT domain do not participate in V_m regulation. However, shortening of the CT to the minimum length that still retains channel-forming ability (23) by the mutation G242stop almost completely abolished g_j dependence on V_m (Fig. 1*A* G242stop) whereas V_j gating did not change significantly. The conductance of hybrid junctions comprised of G242stop hemichannels on one side and WT hemichannels in the other cell was V_m sensitive, but the sensitivity of G_{jss} was intermediate between those of the respective homotypic junctions (Fig. 1*C*). The G_{jss}/V_m relation for G242stop-WT junctions was well fit by a single Boltzmann function with parameters close

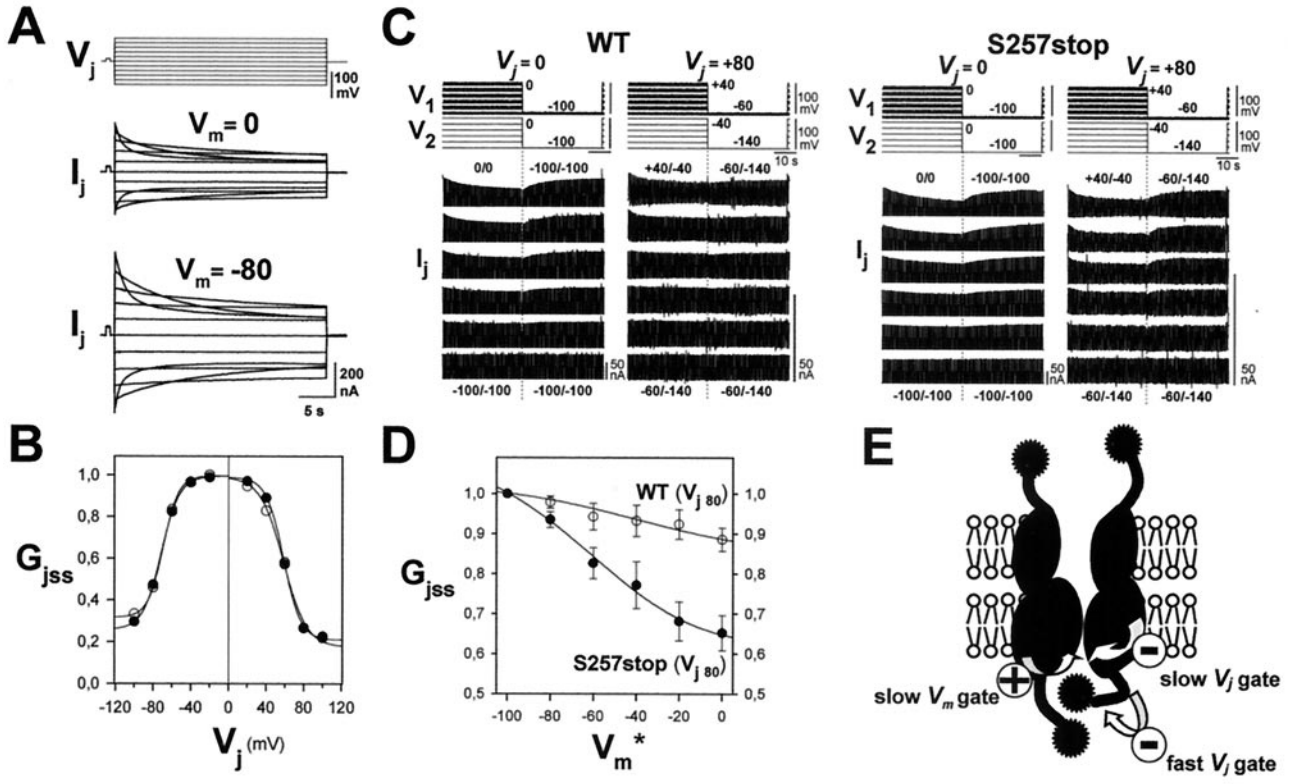

Fig. 3. Interactions between V_j and V_m gating. *(A)* Effect of V_m on V_j dependence. Records of junctional currents (I_j) elicited by the same V_j steps (±100 mV by 20 mV increments and 30 s duration) applied at two holding potentials (V_m = 0 and −80 mV). The V_m difference changed junctional conductance from $g_{j(0\ mV)}$ = 2.72 μS to $g_{j\ (-80\ mV)}$ = 4.80 μS, but the junctional currents declined for increasing positive and negative V_j steps with similar characteristics (positive I_j are shown upward). *(B)* Plots of G_{jss}/V_j relations normalized to g_j at 0 (○) and −80 mV (●) were essentially superimposable, indicating that V_j gating was little affected by V_m. *(C)* Effect of V_j on V_m dependence. Sample records of junctional currents (I_j) after subtraction of nonjunctional currents evoked by the same V_m protocol as in Fig. 1 for V_j = 0 (left) and V_j = +80 mV (right) in pairs expressing WT and truncated S257stop junctions. Conductances at the two holding potential were $g_{j(V_j}$ = 0) = 8.31 and $g_{j(V_j}$ = 80) = 1.57 μS for WT junctions and $g_{j(V_j}$ = 0) = 10.81 to $g_{j(V_j}$ = 80) = 1.27 μS for S257stop junctions. With V_j = 0 mV, equal depolarization of both cells equally decreased g_j of WT and of S257stop junctions. However, when g_j was reduced at V_j = +80 mV, V_m sensitivity of WT junctions was markedly reduced, whereas sensitivity of S257stop junctions in which the fast V_j gate was removed (18) was little affected. For comparison, current gains are increased for the V_j = +80 mV records. *(D)* G_{jss}/V_m relations of WT (○) and truncated S257stop (●) junctions for V_j = +80 where G_j is normalized to the value at V_m*. The curves are fits of the squared Boltzmann relations with parameters of Table 1. Each point represents mean values (±SEM) of four pairs. *(E)* Gating model for the combined V_j and V_m dependence of Cx43 junctions. See *Discussion*.

to those used in the squared Boltzmann relation to describe the behavior of homotypic WT junctions (Table 1). This result suggests that the V_m dependence of the hybrid junctions was due to the single V_m gate contributed by the WT hemichannels, a conclusion previously reported for other hybrid junctions (10, 14). Taken together, these results strongly suggest that the CT region between 242–257 contains residues required for V_m dependence of RCx43 junctions.

Table 1. Boltzmann parameters for V_m-dependence of WT and mutant RC×43 junctions

	A, mV^{-1}	n, 20°C	V_0, mV	G_{jmax}	G_{jmin}	P_{omin}
WT/WT (V_j = 0)*	0.043	1.09	−54	1.03	0.78	0.61
WT/WT (V_j = 80)*	0.031	0.79	−38	1.01	0.92	0.85
S257stop/S257stop (V_j = 0)*	0.041	1.06	−59	1.04	0.79	0.62
S257stop/S257stop (V_j = 80)*	0.037	0.94	−62	1.05	0.77	0.59
G242stop/G242stop	NE	NE	NE	NE	NE	NE
G242stop/WT†	0.046	1.16	−60	1.02	0.81	—
R243Q + D245Q/R243Q + D245Q*	NE	NE	NE	NE	NE	NE
R243Q/R243Q*	0.027	0.69	+11	1.04	0.91	0.83
D245Q/D245Q*	0.059	1.48	−64	1.04	0.41	0.64

*G_{jss}/V_m relations of homotypic junctions were described by the square of a Boltzmann relation, based on a model of two independent V_m gates in series, one in each hemichannel, where each gate could be either open or completely closed.

†The G_{jss}/V_m relation of the heterotypic G242stop-WT junctions was fit by a single Boltzmann relation, assuming that only the gate of the WT hemichannels was contributing to the V_m sensitivity; the calculated parameters were close to those of the WT gate obtained by fitting a squared Boltzmann. NE, not estimated; the changes in G_{jss} were too small to allow accurate determination of the parameters. However, the smooth curves for these junctions in Figs. 1–3 were obtained by the same fitting procedures as for the more sensitive junctions.

Identification of Residues that Participate in V_m Sensing. The loss of V_m sensitivity caused by the truncation of the CT domain at position 242 but not at position 257 may be due to loss of charged residues that contain or contribute to the V_m sensor. Remarkably, there are only two charged residues in the primary sequence of RCx43 in this region, positively charged Arg-243 and negatively charged Asp-245 (Fig. 2*A*). To investigate the role of these charges, we engineered full-length Cx43 in which one or both of these amino acids were replaced by glutamine, a polar uncharged residue. The double neutralization, R243Q and D245Q, virtually abolished V_m dependence (Fig. 2*B* R243Q+D245Q and 2*C*), whereas the D245Q mutation increased sensitivity and the R243Q mutation decreased it, but not to the extent of the double mutation (Figs. 2*B* R243Q and D245Q *and* 2*C*). These data indicate that Arg-243 and Asp-245 are required for Cx43 channels to sense V_m. The single neutralization of the positively charged residue, R243Q, reduced V_m dependence and decreased the equivalent gating charge (Table 1). Conversely, neutralization of the negatively charged residue (D245Q) increased V_m dependence and increased the equivalent gating charge by a similar amount. The R243Q mutation moved V_0 in the positive direction whereas the D245Q mutation shifted V_0 to a more negative value**,** as appropriate for the changes in gating charge (Fig. 2*C Inset*). The single and double neutralizations had little if any effect on V_j dependence of g_j (illustrated in supplementary text and supplementary Fig. 4, which are published as supplemental data on the PNAS web site, www.pnas.org).

Interactions Between V_m Gating and V_j Gating. Because truncation at residue 257 affects V_j sensitivity (18), and truncation at nearby residue 242 blocks V_m sensitivity with no further change in V_j sensitivity, we investigated whether V_j and V_m gating interact. At V_m values of −80 and 0 mV at which G_{jss} differed almost 2-fold, V_j gating was virtually the same (Fig. 3*A* and *B*). The kinetics was not distinguishably different, and the steady state G_{jss}/V_j relations, normalized to the different values of g_j at $V_j = 0$, also were little affected. These data indicate that V_j gating operates independently of V_m gating. Previously, mouse Cx45 junctions were shown to have very similar V_j gating at different V_m values that changed g_j on depolarization by a factor of 2.5 (10).

We also studied V_m gating in the presence of a fixed, non-zero V_j. Cx43 junctions are particularly suitable for this kind of analysis because the residual conductance or V_j-insensitive component is large enough to allow estimation of V_m effects at large V_j's. For the example of Fig. 3, we defined $V_m^* = (V_1 + V_2)/2$ and examined V_m^* dependence for $V_j = +80$ mV from $V_m^* = -100$ mV to 0 mV. A V_j of +80 mV at $V_m^* = -100$ mV, i.e., $V_1 = -60$ mV and $V_2 = -140$ mV, decreased conductance to a value very close to the V_j-insensitive component (Fig. 3*B*). Equal depolarization of both cells induced an additional reduction in g_j, but the sensitivity to V_m was reduced somewhat more than would result from block of a single V_m gate (Figs. 3*C* WT and 3*D*). Thus, the presence of a large V_j appears to interfere with operation of both V_m gates. To explore this interaction further, we carried out the same experiment evaluating the effect of a maintained V_j on V_m dependence in S257stop–S257stop junctions, which lack fast V_j gating (18). Furthermore, G_{jmin} was markedly smaller for these mutant junctions than for wild type, 0.16 vs. 0.36 respectively for $V_j < 0$ and 0.13 vs. 0.24 for $V_j > 0$. The G_{jss}/V_m relation was little affected by this mutation (Figs. 1*A* S257stop and 1*C*; Fig. 3*C* S257stop left). Moreover, when g_j was decreased by a V_j of +80 mV, the fractional change in g_j was the same as in the absence of V_j gradient (Figs. 3*C* S257stop right and 3*D*). Thus, truncation at 257, which abolished the fast V_j gating, restored V_m gating in the presence of V_j.

Discussion

Structure–Function Analysis of V_m Dependence of Cx43 Channels. We identified two charged residues, Arg-242 and Asp-245, that are likely to be an integral part of the V_m sensor and that are located in the (cytoplasmic) CT domain close to its junction with M4, the fourth transmembrane domain. Mutations of these residues that altered V_m gating did not have any influence on V_j gating, and the S257stop truncation that greatly modified V_j gating did not affect V_m sensitivity. Taken together along with the difference in residual conductance, G_{jmin}, the results indicate that V_m and V_j regulation of Cx43 junctional conductance is mediated by separate but interacting domains.

Truncation by the mutation G242stop greatly reduced V_m sensitivity whereas truncation by S257stop had little effect on this property. Only two of the residues between positions 242 and 257 are charged, Arg-243 and Asp-245. When the acidic residue was replaced by Gln, a neutral amino acid, the G_{jss}/V_m relation was increased in steepness and V_0 was shifted in the negative direction, suggesting that D245 is part of the V_m sensor. When the basic residue was replaced by Gln (R243Q), the G_{jss}/V_m relation was decreased in steepness and V_0 was shifted in the positive direction, suggesting that R243 is also part of the V_m sensor and that it moves in the same direction as D245 during V_m gating. However, the effects of the two mutations did not summate, and the double mutation, which is electrically neutral, virtually abolished V_m dependence. Apparently the double mutation caused structural changes that prevented V_m gating. Although the anatomical symmetry of gap junctions suggests that there are two V_m gates in series, a single Boltzmann relation fit the G_{jss}/V_m relation about as well as the squared Boltzmann relation (with different parameters). However, the heterotypic junctions WT-G242stop would be expected to have only one V_m sensitive gate, and the single Boltzmann with the same parameters as for the squared Boltzmann applied to WT junctions gave an excellent fit. This observation is strong evidence for series V_m gates and applicability of the squared Boltzmann to WT junctions.

A Novel Gating Model for Connexin Channels with Combined V_j and V_m Dependence. A model for the actions of V_j and V_m on Cx43 channels can be derived from data obtained in this paper and a previous analysis of the V_j dependence (18). We hypothesize that each hemichannel contains a set of three gates, one fast gate and one slow gate under V_j control and one slow gate regulated by V_m (Fig. 3*D*). The three gates appear to involve different regions of the connexin molecule, because they can be modified independently by different mutations and their residual conductances are different. The distal part of CT domain is involved in the fast V_j gating process, because deletion of the 257–382 region modified the time course of g_j transitions from a two-component decay to a single-component with a slow time constant. Block of the fast component by the 257 truncation and the asymmetry of the G_{jss}/V_j relation in heterotypic WT-S257stop junctions suggest that there are two V_j gating mechanisms within the hemichannel, each operating with the same negative polarity of closing, defined as relative negativity in cytoplasmic side (18). The distal end of the CT may move to partially occlude the channel during fast V_j gating as has been proposed for pH gating (24). Interestingly, attachment of aequorin (25) or of enhanced green fluorescent protein (EGFP; ref. 26) to the CT of a full-length Cx43 blocks fast V_j gating. The mutations Arg-243 and Asp-245 affecting V_m gating also are located in the CT but more proximal to the region required for fast V_j gating. In the absence of V_j gradients, Cx43 conductance is exclusively dependent on V_m, which induces closure by membrane potential depolarization. When the CT domain was truncated at position 242, fast V_j and V_m gating were blocked, but the slow V_j gating seen in the

S257stop mutant was little affected. In Cx43 junctions, the sensor for the slow mechanism of V_j gating may correspond to those initially proposed for Cx32 and Cx26 junctions, where the charged amino acids located in the NT domain and at the beginning of the first extracellular loop determine the polarity of closing of the channels (15, 17).

In this model, G_j should be governed by the combined action of three gating mechanisms according to their kinetic properties and their polarity of closing. Moreover, the effects on conductance will be also determined by the nature of interactions between the gating mechanisms, which will depend critically on their structural basis and where they are located with respect to each other and to the channel lumen. Interactions could be allosteric or could result from changes in the local electric field by the gating mechanisms. The fast and slow V_j gates may interact electrically. At large V_j, the fast V_j component dominates the conductance change of WT junctions, and G_{jmin} was larger than in S257stop junctions. This result suggests that the fast gate has a larger residual conductance and prevents closure of the slow gate. That the time constants for the 257 truncation mutant are somewhat shorter than for the slow component in the WT may result from a larger voltage across the sensor in the absence of the fast gating mechanism. Operating in a different time regime, a large value of V_j that closes most V_j gates modifies V_m gating, and it appears that the V_m gate does not operate when the V_j gate is closed (Fig. 3 *C* and *D*). (See supplemental material for further discussion of V_j–V_m interactions.)

Single channel analysis of the gating mechanisms should reveal the classes of gating events, including their probabilities, residual conductances, and intervening states. V_j induces fast transitions between fully or partially open states and residual states of low conductance (27). In addition, slow transitions to a fully closed state have been recorded at larger V_j in WT junctions (28). These two kinds of transition presumably underlie the two types of V_j sensitivity considered here. In Cx43-EGFP junctions, which lack fast V_j gating, fast transitions to a residual open state are not present, and channels close fully by slow transitions (26). The events in V_m gating have not yet been observed at the single channel level, but the ability of V_m to further reduce the V_j-insensitive component of macroscopic conductance is an indication that V_m gating mediates transitions between open and fully closed states of channels. Full closure of the channels is also suggested by the fact that the V_j gating properties of Cx43 (Fig. 3 *A* and *B*) do not change significantly at different membrane potentials although the V_m induces large variations in macroscopic junctional conductance. If V_m gates closed to a subconductance state, one would be expected that the voltage across the V_j gates would change affecting kinetics and steady state values.

The model presented here may be applicable in whole or in part to other V_m- and V_j-sensitive gap junctions of vertebrates (11, 14). The dependence on V_m in some vertebrate junctions is sufficiently great that intercellular coupling could be directly regulated by the membrane potential, a parameter that is always present and that varies, particularly in excitable cells. Dynamic changes of coupling coefficient in phase with membrane potential oscillations occur in pancreatic β-cells (29), which may indicate that the conductance of those junctions is V_m dependent. V_j gating would regulate coupling when membrane potentials differed, as in asynchronously active excitable cells.

We thank E. C. Beyer for providing rat Cx43 cDNA. We gratefully acknowledge Rosa Barquero for technical assistance. This work was supported by a grant of the European Community (QLG1-CT-1999-00516 to L.C.B.). M.V.L.B. is supported by National Institutes of Health Grant NS-07512 and is the Sylvia and Robert S. Olnick Professor of Neuroscience.

1. Unger, V. M., Kumar, N. M., Gilula, N. B. & Yeager, M. (1999) *Science* **283,** 1176–1180.
2. Bruzzone, R., White, T. W. & Paul, D. L. (1996) *Eur. J. Biochem.* **238,** 1–27.
3. Bennett, M. V. L. & Verselis, V. K. (1992) *Semin. Cell Biol.* **3,** 29–47.
4. Obaid, A. L., Socolar, S. J. & Rose, B. (1983) *J. Membr. Biol.* **73,** 69–89.
5. Verselis, V. K., Bennett, M. V. L. & Bargiello, T. A. (1991) *Biophys. J.* **59,** 114–126.
6. Bukauskas, F. F., Kempf, C. & Weingart, R. (1992) *J. Physiol. (London)* **448,** 321–337.
7. Churchill, D. & Caveney, S. (1993) *J. Membr. Biol.* **135,** 165–180.
8. Phelan, P., Stebbing, L. A., Baines, R. A., Bacon, J. P., Davies, J. A. & Ford, C. (1998) *Nature (London)* **391,** 181–185.
9. White, T. W., Bruzzone, R., Wolfram, S., Paul, D. L. & Goodenough, D. A. (1994) *J. Cell Biol.* **125,** 879–892.
10. Barrio, L. C., Capel, J., Jarillo, J. A., Castro, C. & Revilla, A. (1997) *Biophys. J.* **73,** 757–769.
11. Manthey, D., Bukauskas, F., Lee, C. G., Kozak, C. A. & Willecke, K. (1999) *J. Biol. Chem.* **274,** 14716–14723.
12. Verselis, V. K., Bargiello, T. A., Rubin, J. B. & Bennett, M. V. L. (1993) *Prog. Cell Res.* **3,** 97–104.
13. Zhao, H. B. & Santos-Sacchi, J. (2000) *J. Membr. Biol.* **175,** 17–24.
14. Barrio, L. C., Revilla, A., Gómez-Hernández, J. M., de Miguel, M. & González, D. (2000) in *Gap Junctions: Molecular Basis of Cell Communication in Health and Disease*, ed. Peracchia, C. (Academic, San Diego), pp. 175–188.
15. Verselis, V. K., Ginter, C. S. & Bargiello, T. A. (1994) *Nature (London)* **368,** 348–351.
16. Ri, Y., Ballesteros, J. A., Abrams, C. K., Oh, S., Verselis, V. K., Weinstein, H. & Bargiello, T. A. (1999) *Biophys. J.* **76,** 2887–2898.
17. Oh, S., Rubin, J. B., Bennett, M. V. L., Verselis, V. K. & Bargiello, T. A. (1999) *J. Gen. Physiol.* **114,** 339–364.
18. Revilla, A., Castro, C. & Barrio, L. C. (1999) *Biophys. J.* **77,** 1374–1383.
19. Beyer, E. C., Paul, D. L. & Goodenough, D. A. (1987) *J. Cell. Biol.* **105,** 2621–2629.
20. Barrio, L. C., Suchyna, T., Bargiello, T. A., Xu, L. X., Roginski, R. S., Bennett, M. V. L. & Nicholson, B. J. (1991) *Proc. Natl. Acad. Sci. USA* **88,** 8410–8414.
21. Spray, D. C., Harris, A. L. & Bennett, M. V. L. (1981) *J. Gen. Physiol.* **77,** 77–93.
22. Harris, A. L., Spray, D. C. & Bennett, M. V. L. (1981) *J. Gen. Physiol.* **77,** 95–117.
23. Dunham, B., Liu, S., Taffet, S., Trabda-Janik, E., Delmar, M., Tetryshyn, R., Zheng, S., Perzova, R. & Vallano, M. L. (1992) *Circ. Res.* **70,** 1233–1243.
24. Morley, G. E., Taffet, S. M. & Delmar, M. (1996) *Biophys. J.* **70,** 1294–1302.
25. Martin, P. E. M., George, C. H., Castro, C., Kendall, J. M., Capel, J., Campbell, A. K., Revilla, A., Barrio, L. C. & Evans, W. H. (1998) *J. Biol. Chem.* **273,** 1719–1726.
26. Bukauskas, F. F., Jordan, K., Bukauskiene, A., Bennett, M. V. L., Lampe, P. D., Laird, D. W. & Verselis, V. K. (2000) *Proc. Natl. Acad. Sci. USA* **97,** 2556–2561. (First Published March 7, 2000; 10.1073/pnas.050588497)
27. Moreno, A. P., Rook, M. B. & Spray, D. C. (1994) *Biophys. J.* **67,** 113–119.
28. Banach, K. & Weingart, R. (2000) *Pflügers Arch. Eur. J. Physiol.* **439,** 248–250.
29. Andreu, A., Soria, B. & Sanchez-Andres, J. V. (1997) *J. Physiol. (London)* **498,** 753–761.